

Short time scales of magmatic assimilation from diffusion modeling of multiple elements in olivine

Fidel Costa*

Institut für Geologie, Mineralogie, und Geophysik, Ruhr-Universität-Bochum, Bochum 44780, Germany

Michael Dungan

Section of Earth Sciences, University of Geneva, 13 rue des Maraîchers, Geneva, Switzerland

ABSTRACT

Open-system processes have a large capacity to modify magma compositions during differentiation. Obtaining the rates of such processes is essential to understanding and constraining the evolution of magmatic systems. Here we quantify the time scales for magmatic assimilation of hydrous mafic to ultramafic cumulates by ascending basalts using the zoning patterns of olivine xenocrysts. Robust diffusion modeling results have been obtained by treating multiple compositional profiles for multiple elements (Fe-Mg, Ni, Mn, Ca) on multiple crystals from multiple flows. We find that the time between assimilation and eruption ranges from a few months to ~25 yr, although 80% of the results are <10 yr. These ranges are shorter than either magma transport times from the mantle to the surface or typical repose periods of arc volcanoes. Thus, modification of the geochemical and mineralogical features of basalts by assimilation of plutonic rocks is a fast and probably unavoidable magmatic process.

Keywords: diffusion, olivine, assimilation, magma, time scales.

INTRODUCTION

The rates of geological processes implicated in magma generation and evolution are still poorly known despite their importance for quantifying magmatic systems (e.g., Reid, 2003; Hawkesworth et al., 2004). Constraints on the timing and duration of magma migration at shallow levels have been obtained for a few active volcanoes, mainly using real-time geophysical monitoring (e.g., White, 1996). Diverse applications of U-series disequilibria to the study of magmatic rates and residence times are proving to be extremely powerful (e.g., Condomines et al., 2003; Turner et al., 2003), but young eruptive ages (<300 ka) are an absolute necessity.

Kinetic modeling of chemical gradients in minerals provides an alternative chronological tool that can access a large range of time scales and can be applied to rocks of any age (e.g., Jurewicz and Watson, 1988; Nakamura, 1995; Zellmer et al., 1999; Coombs et al., 2000; Klügel, 2001; Pan and Batiza, 2002; Costa et al., 2003; Morgan et al., 2004; Costa and Chakraborty, 2004; Shaw, 2004). Compositional profiles across zoned grains obtained with in situ analytical techniques can be used to determine the residence times of such crystals at magmatic temperatures if the relevant diffusion rates are available and if the processes responsible for zoning can be in-

dependently established. In this way one can directly link the temporal information with the magmatic process recorded in the mineral.

Here we model the compositions of olivines from a sequence of 30 basaltic lava flows, the Upper Placeta San Pedro sequence (235 ka; Tatara-San Pedro complex, 36°S, Chilean Andes; Dungan et al., 2001), to establish the time scales of partial assimilation of mafic to ultramafic lithologies by basaltic magmas (e.g., Kelemen, 1986; Dungan and Davidson, 2004). These olivine xenocrysts are the remnants of partially melted and disaggregated xenoliths. The chemical impact of assimilation of the xenoliths and their grain-boundary partial melts is manifested by large but poorly correlated variations in both compatible and incompatible elements in these lavas (e.g., Figs. 19–20 of Dungan et al., 2001; Fig. 2 of Dungan and Davidson, 2004).

TEXTURAL AND MINERALOGICAL OBSERVATIONS

Evidence for and Implications of a Xenocrystic Origin of Olivine Crystals

Many of the Upper Placeta San Pedro lavas are 10–20 m thick and contain microxenolithic fragments (3–10 mm) that are characterized by plutonic textures (e.g., Fig. 1 of Dungan and Davidson, 2004). A typical feature of olivine xenocrysts (diameters of ~250–2000 μm) and some augites is the presence of healed microfractures that apparently reflect a subsolidus history. These are also present in

Miocene gabbroic xenoliths of Volcán San Pedro (Costa et al., 2002). Many of the olivines in these lavas have embayed morphologies wherein channels are filled with Mg- and alkali-rich mineral assemblages (Dungan and Davidson, 2004). The large single crystals and multigrain clots in lavas are interpreted as being derived from initially much larger partially melted and disaggregated xenoliths of mafic to ultramafic cumulates.

Xenocrystic olivines display decreasing Fo contents [$\text{Fo} = (100 \cdot \text{Mg}) / (\text{Mg} + \text{Fe}_{\text{tot}})$, Fe_{tot} = total iron, in mols] toward crystal margins (Fig. 1). Core plateaus range from Fo_{84} to Fo_{79} . Rim compositions vary depending on whether they are in contact with basaltic groundmass (Fo_{72-68}), or terminate at channels containing the alkali- and Mg-rich assemblage (Fo_{76-72}). Olivine appears to have been stable in these magmas until eruption, because some samples contain minor groundmass olivine (Fo_{70-68}). The core compositions of small olivine phenocrysts (<150 μm , Fo_{81-77}) in the weakly contaminated basalts overlap with the xenocrysts. NiO profile shapes are similar to those of Fo, whereas MnO and CaO show core plateaus and increasing concentrations toward crystal rims (Fig. 1).

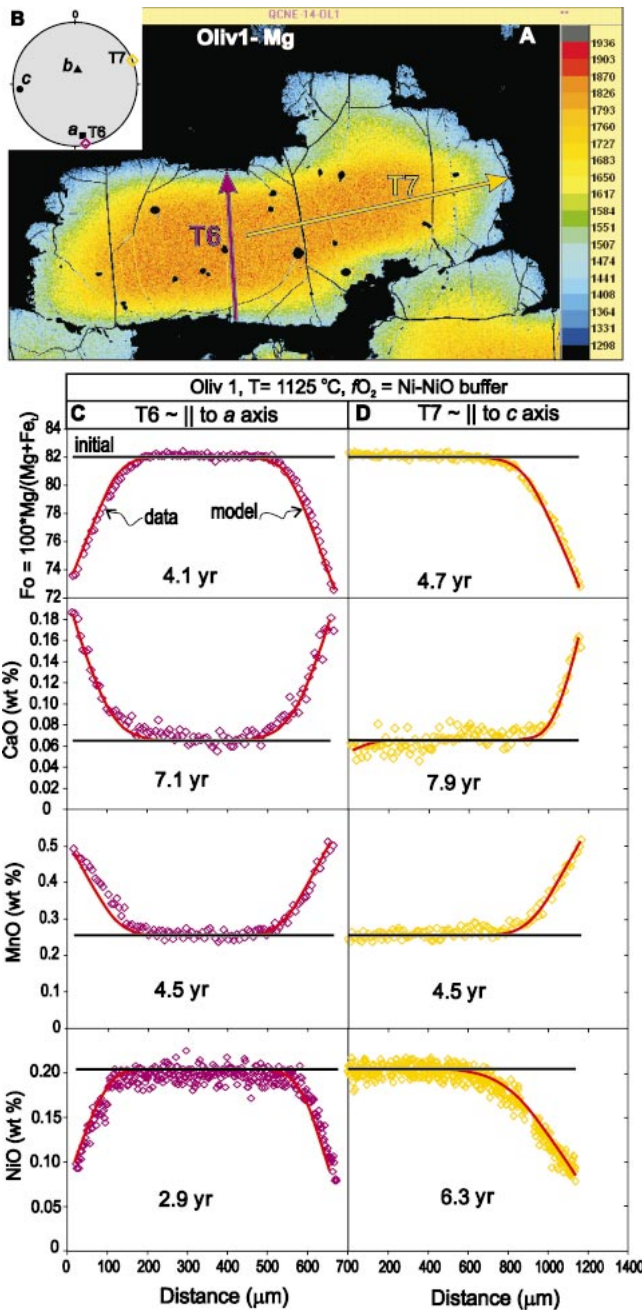
APPROACH TO DIFFUSION MODELING

Diffusion Equation, Initial and Boundary Conditions

Because the diffusion rates of Fe, Mg, Mn, and Ni in olivine are dependent on Fo content,

*Corresponding author: E-mail: Fidel.Costa-Rodriguez@rub.de.

Figure 1. Example of zoning patterns and modeling results from Oliv1 of sample QCNE.14. **A:** X-ray map of Mg concentration in Oliv1. Arrows T6 and T7 mark positions of electron microprobe traverses for which data and modeling results are shown in C and D, respectively. Asymmetric zoning in this olivine shows effect of more rapid Fe-Mg diffusion parallel to *c* axis (approximately parallel to T7) compared to parallel to *a* axis (approximately parallel to T6) and effect of diffusion in two dimensions (e.g., upper margin above T7). **B:** Crystallographic axis orientations for Oliv1 and electron microprobe traverses projected onto lower hemisphere. **C and D:** Concentration profiles for traverses T6 and T7 showing measured concentrations, initial conditions, model profiles, and calculated times for 1125 °C and f_{O_2} at NNO buffer. Results of two traverses for all elements overlap at 5.4 ± 2.5 yr. This suggests that zoning patterns are due to diffusive exchange, that assumption of initial profiles is appropriate, and that diffusion coefficients are correct.



we have used the following form of Fick's Second Law for these elements (1 dimension):

$$\frac{\partial C}{\partial t} = \frac{\partial}{\partial x} \left(D \frac{\partial C}{\partial x} \right), \quad (1)$$

where C is concentration, t is time, D is the diffusion coefficient, and x is distance. As the experimental data for Ca do not record a dependence on Fe/Mg (see following), a compositional term was not included for Ca. We used the following initial (2) and boundary (3) conditions:

$$C = C_0, \quad t = 0, \quad (2)$$

$$C(r) = C_1, \quad t > 0, \quad (3)$$

where r is the coordinate corresponding to the rim of the crystal. Condition 3 expresses the fact that we have used a constant composition (e.g., time invariant, C_1) at the rims. Initial conditions in which the olivine xenocrysts were uniform in composition (C_0) are supported by their volumetrically significant core plateaus. The near absence of zoning in such cores is probably due to long plutonic residence times during which olivine equilibrated with adjacent minerals. The variations in core plateau compositions between and within samples are consistent with entrainment of xenocrysts from compositionally diverse plutonic lithologies (Costa et al., 2002), and this variability does not compromise our approach. The boundary condition for the diffusion

calculation is taken as the composition at the edge of the crystal (condition 3). Uncertainties about the boundary conditions could arise because the olivine experienced an initial dissolution event during partial melting of the inferred gabbroic sources. However, as long as the dissolution event was fast (Dungan, 2005), this would only erase zoning at the olivine rims inherited from a plutonic history. Thus, with our approach we only consider the immersion time of olivines in host melts after grain-boundary melting and xenolith disaggregation.

Diffusion Coefficients, Anisotropy, and the Effect of More than One Dimension

Experimental determinations of cation diffusivities in olivine show that they depend on temperature (T), oxygen fugacity (f_{O_2}), crystallographic direction, and composition (Fe and Mg—Chakraborty, 1997; Dohmen et al., 2003; Ni and Mn—Petty et al., 2004; Ca—Coogan et al., 2005). The diffusion rates of these elements depend on Fo content, except for Ca, which within Fo_{90-83} is independent of Fe-Mg (Coogan et al., 2005). The dependence on (f_{O_2}) decreases in the order $Ca > Ni > Fe-Mg \sim Mn$. Anisotropy of diffusion is strong and of similar magnitude for Fe-Mg, Mn, and Ni, for which diffusion parallel to the c axis is approximately six times faster than parallel to the a or b axis, whereas for Ca, diffusion parallel to the c axis is only approximately two times faster than to the a or b axis. The expressions that we have used for the diffusion coefficients can be found in the Data Repository.¹

Following Costa and Chakraborty (2004), we have modeled diffusion anisotropy by determining the D parallel to the traverses after obtaining the orientations of the olivine crystallographic axes by electron backscatter diffraction (at Ruhr-Universität Bochum). Most electron microprobe traverses (Cameca SX-50, University of Lausanne and Ruhr-Universität Bochum) of olivine were done parallel to one crystal face. We commonly made more than one traverse in the same crystal, and we also obtained X-ray maps to establish the zoning patterns in two dimensions (Fig. 1).

Accounting for the effects of diffusion in more than one dimension is essential to retrieval of accurate times (Costa et al., 2003; Costa and Chakraborty, 2004). Crystal shapes and X-ray maps were used to select traverses that are least affected by diffusion in two di-

¹GSA Data Repository item 2005165, Expressions for the diffusion coefficients, is available online at www.geosociety.org/pubs/ft2005.htm, or on request from editing@geosociety.org or Documents Secretary, GSA, P.O. Box 9140, Boulder, CO 80301-9140, USA.

mensions (Fig. 1A). Uncertainties arising from diffusion in the third dimension were minimized by excluding crystals for which the olivine *c* axis is highly oblique with respect to the plane of the thin section (see Costa and Chakraborty, 2004). Of 130 traverses, 57 passed these tests and have been modeled for Fe-Mg.

Effects of Temperature and Oxygen Fugacity Plus Uncertainties

Critical parameters for retrieving time information from olivine compositional profiles are *T* and f_{O_2} . We have constrained a *T* range of the basalts using the MELTS algorithm (Ghiorso and Sack, 1995) and the composition of the least contaminated lava (sample QTW11.36, no. 106, in Table 2f of Dungan et al., 2001) at an f_{O_2} typical for arc mafic magmas (NNO buffer, Huebner and Sato, 1970) and over a range of water contents (1–5 wt% H₂O) and pressures (*P*, 0.1–0.6 GPa), for which we obtained liquidus temperatures (T_L) between 1175 and 1120 °C. Phenocryst and groundmass core compositions of olivine (Fo_{83–80}) and plagioclase (An_{85–80}) and the absence of pyroxene phenocrysts in this sample are most closely reproduced at 0.2–0.3 GPa (2–3 wt% H₂O) and *T* 1120–1145 °C. Because assimilation and diffusive equilibration of xenocrysts occurred over a *P-T* range below the T_L during magma ascent, we chose a *T* range of 1100–1150 °C, and we report calculated times for a mean *T* of 1125 °C because most of the diffusion must have occurred at the high end of the temperature range (Figs. 1C, 1D, and 2C).

Uncertainties in the calculations are related to estimates of *T* and f_{O_2} . Varying *T* over 1100–1150 °C changes *D* by a factor of 3.5 for Fe-Mg to a maximum of 5.5 for Ca (Fig. 2A), and a change of two log units in f_{O_2} at 1125 °C (NNO-1 to NNO+1; Fig. 2B) causes *D* to vary by a factor of 2 for Fe-Mg up to a maximum of 4 for Ca. Experimental uncertainties for the diffusion coefficients that we have used could change our calculated times by a factor of two. The consistent results from modeling multiple elements in a single crystal (Fig. 1) lead to a confidence level that is higher than the preceding discussion would suggest.

MODELING RESULTS AND GEOLOGICAL IMPLICATIONS

Using the strategy outlined here we have modeled the Fe-Mg concentrations for 57 traverses from 25 crystals plus the Ni, Ca, and Mn concentrations for 2 traverses on a single crystal using the finite differences numerical technique. These results bear not only on the time scales of magmatic processes but also on the validity and robustness of the approach.

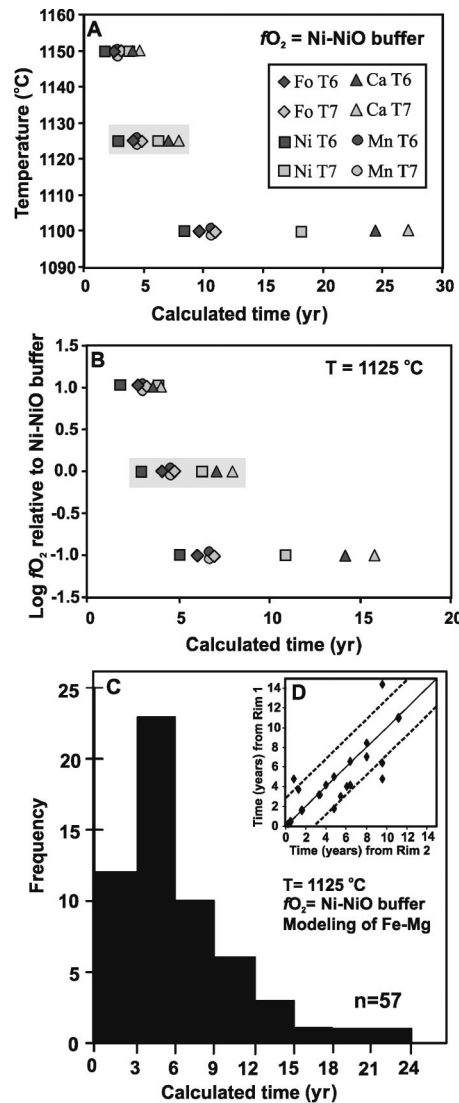


Figure 2. A: Effect of temperature on calculated times for Oliv1-QCNE.14. Range of calculated times decreases with increasing temperature. Gray field highlights temperature used for calculations. **B:** Increasing f_{O_2} decreases range and absolute values of calculated times. Gray field highlights f_{O_2} used for calculations. **C:** Histogram of calculated crystal residence times (at 1125 °C and NNO) from modeling Fe-Mg chemical gradients in olivines from Upper Placeta San Pedro sequence lavas. **D:** Comparison of calculated times using two rims of same crystal. Note that many crystals show same time for both rims (fall on line with slope of 1) and most of rest show maximum difference of 3 yr between opposite rims (dotted lines).

Modeling Results: Consistent Time Determinations from Multiple Elements and Olivine Crystals

The results of modeling Ni, Ca, Mn, and Fe-Mg from two nearly perpendicular traverses (T6 and T7), each of which is parallel to a different crystallographic axis (*a* and *c*, respectively) in a single crystal, show remarkable agreement (Fig. 1). Virtually identical

times for the two traverses are calculated for Fe-Mg ($T_6 = 4.1$ and $T_7 = 4.7$ yr), Mn (4.5 yr), and Ca (7.1 and 7.9 yr). The times calculated from Ni (2.9 and 6.3 yr) show a greater dispersion, but are still within the error of the *D* (Petry et al., 2004). The times determined with different elements overlap within 5.4 ± 2.5 yr. The results from modeling Fe-Mg concentrations from all crystals vary between ~2 months and ~22 yr, but (1) there is a prominent mode between 3 and 6 yr (Fig. 2C), and ~80% of the times are <10 yr, and (2) opposite rims of the same crystal commonly yield consistent results (Fig. 2D). Thus, Fe-Mg modeling in many crystals agrees with our more detailed analysis of multiple elements in Oliv1 (Fig. 1). The overall spread of a few months to ~25 yr could in part arise from cryptic geometric irregularities, but there is certainly a natural range in residence times of different crystals from a single flow. The fact that we calculate somewhat different times for the opposing rims of some crystals (Fig. 2D) could reflect the dynamics of xenolith disaggregation and is consistent with petrographical evidence that the olivines are derived from completely solidified plutons.

The agreement between elements with different diffusion anisotropies and diffusion rates (12 experimentally determined diffusion coefficients were used) would not be observed unless the natural initial and boundary conditions were close to those we have inferred. It follows that diffusive exchange between olivine and host melt is primarily responsible for these zoning patterns. Although crystal growth and probably dissolution are also anisotropic, it is unlikely that they vary by precisely the same factors as the anisotropy of diffusion for multiple elements with different diffusion anisotropies. Jurewicz and Watson (1988) found that olivine dissolution was faster parallel to the *a* than to the *c* axis, which is opposite to the cation diffusion anisotropy and lends support to our assumption that dissolution has a negligible effect on our time determinations. The concordance of the results obtained using diffusion coefficients for Fe-Mg, Ni, Ca, and Mn verifies the accuracy of these determinations within the variability range of our samples.

Geological Implications

Most of the calculated times (Figs. 1 and 2) record short durations of <10 yr for the disaggregation of mafic to ultramafic cumulates in evolved basalt followed closely by eruption. The independent evidence for a subsolidus source of these xenocrystic olivines combined with their short residence times leads to the conclusion that digestion of xenoliths incorporated in basaltic magma is extraordinarily

ly rapid. If thermomechanical barriers to xenolith partial melting and disaggregation are as minimal as these rates imply, it follows that geochemical diversity among and within single eruptive episodes, hence variable overprinting of mantle geochemical signatures related to dispersion of grain-boundary melts and xenocrysts, is potentially common in mafic magmas. For example, the time between partial melting of the mantle and eruption at subduction zones has been proposed to be on the order of hundreds to hundreds of thousands of years on the basis of U-series disequilibria (e.g., Turner et al., 2003). Typical repose periods between eruptions at arc volcanoes range from decades to millennia. Thus, it seems that there is ample time for arc magmas to assimilate even refractory mafic to ultramafic lithologies.

Broader implications and applications of our study are that modeling the chemical gradients in igneous minerals can provide a unique window into the time scales and rates of magmatic process. In particular, modeling multiple elements in multiple traverses from multiple olivine crystals provides an unprecedented level of precise, consistent, and robust time estimates on rocks of any eruption age, which is impossible to achieve by any isotopic method. Combining this approach with mineral dissolution data (e.g., Edwards and Russell, 1998) and detailed thermodynamical models (Ghiorso and Sack, 1995; Spera and Bohrsen, 2004) should increase our understanding of how magmatic systems work and constrain the time pathways along which they function.

ACKNOWLEDGMENTS

Costa acknowledges many enlightening and exciting discussions with S. Chakraborty about the many aspects of diffusion. We thank R. Dohmen for discussions and help in computer modeling, and L. Coogan for suggestions that improved the clarity of the manuscript and for allowing us to use his unpublished data. Reviews by J.K. Russell, G. Zellmer, and N.L. Green are acknowledged. Costa is supported by the Deutsche Forschungsgemeinschaft under the SFB 526 program. Dungan is supported by Swiss National Science Foundation grant 20-103731.

REFERENCES CITED

- Chakraborty, S., 1997, Rates and mechanisms of Fe-Mg interdiffusion in olivine at 980 °C–1300 °C: *Journal of Geophysical Research*, v. 102, p. 12,317–12,331, doi: 10.1029/97JB00208.
- Condomines, M., Gauthier, P.-J., and Sigmarsson, O., 2003, Timescales of magma chamber processes and dating of young volcanic rocks, in Bourdon, B., et al., eds., *Uranium series geochemistry: Reviews in Mineralogy and Geochemistry*, v. 52, p. 125–174.
- Coogan, L.A., Hain, A., Stahl, S., and Chakraborty, S., 2005, Experimental determination of the diffusion coefficient for calcium in olivine between 900 °C and 1500 °C: *Geochimica et Cosmochimica Acta* (in press).
- Coombs, M.L., Eichelberger, J.C., and Rutherford, M.J., 2000, Magma storage and mixing conditions for the 1953–1974 eruptions of Southwest Trident volcano, Katmai National Park, Alaska: *Contributions to Mineralogy and Petrology*, v. 140, p. 99–118, doi: 10.1007/s004100000166.
- Costa, F., and Chakraborty, S., 2004, Decadal time gaps between mafic intrusion and silicic eruption obtained from chemical zoning patterns in olivine: *Earth and Planetary Science Letters*, v. 227, p. 517–530, doi: 10.1016/j.epsl.2004.08.011.
- Costa, F., Dungan, M., and Singer, B.S., 2002, Hornblende- and phlogopite-bearing gabbroic xenoliths from Volcán San Pedro (36°S), Chilean Andes: Evidence for melt and fluid migration and reactions in subduction related plutons: *Journal of Petrology*, v. 43, p. 219–241, doi: 10.1093/petrology/43.2.219.
- Costa, F., Chakraborty, S., and Dohmen, R., 2003, Diffusion coupling between trace and major elements and a model for calculation of magma residence times using plagioclase: *Geochimica et Cosmochimica Acta*, v. 67, p. 2189–2200, doi: 10.1016/S0016-7037(02)01345-5.
- Dohmen, R., Becker, H.-W., and Chakraborty, S., 2003, Point defect equilibration and diffusion in olivine at low temperatures (T<1000 °C): *European Journal of Mineralogy*, v. 15, p. 42.
- Dungan, M., 2005, Partial melting at the Earth's surface: Implications for assimilation rates and mechanisms in subvolcanic intrusions: *Journal of Volcanology and Geothermal Research*, v. 140, p. 193–203, doi: 10.1016/j.jvolgeores.2004.07.021.
- Dungan, M., and Davidson, J., 2004, Partial assimilative recycling of the mafic plutonic roots of arc volcanoes: An example from the Chilean Andes: *Geology*, v. 32, p. 773–776, doi: 10.1130/G20735.1.
- Dungan, M., Wulff, A., and Thompson, R., 2001, A refined eruptive stratigraphy for the Tataras-San Pedro Complex (36°S, Southern Volcanic Zone, Chilean Andes): Reconstruction methodology and implications for magma evolution at long-lived arc volcanic centers: *Journal of Petrology*, v. 42, p. 555–626, doi: 10.1093/petrology/42.3.555.
- Edwards, B., and Russell, J.K., 1998, Time scales of magmatic processes: New insights from dynamic models for magmatic assimilation: *Geology*, v. 26, p. 1103–1106, doi: 10.1130/0091-7613(1998)026<1103:TSOMPN>2.3.CO;2.
- Ghiorso, M.S., and Sack, R.O., 1995, Chemical mass transfer in magmatic processes IV. A revised and internally consistent thermodynamic model for the interpolation and extrapolation of liquid-solid equilibria in magmatic systems at elevated temperatures and pressures: *Contributions to Mineralogy and Petrology*, v. 119, p. 197–212.
- Hawkesworth, C., George, R., Turner, S., and Zellmer, G., 2004, Time scales of magmatic processes: *Earth and Planetary Science Letters*, v. 218, p. 1–16, doi: 10.1016/S0012-821X(03)00634-4.
- Huebner, J.S., and Sato, M., 1970, The oxygen fugacity-temperature relationships of manganese nickel oxide buffers: *American Mineralogist*, v. 55, p. 934–956.
- Jurewicz, A.J.G., and Watson, E.B., 1988, Cations in olivine, Part 2: Diffusion in olivine xenocrysts, with applications to petrology and mineral physics: *Contributions to Mineralogy and Petrology*, v. 99, p. 186–201, doi: 10.1007/BF00371460.
- Kelemen, P.B., 1986, Assimilation of ultramafic rocks in subduction-related magmatic arcs: *Journal of Geology*, v. 94, p. 829–843.
- Klügel, A., 2001, Prolonged reactions between harzburgite xenoliths and silica-undersaturated melt: Implications for dissolution and Fe-Mg interdiffusion rates of orthopyroxene: *Contributions to Mineralogy and Petrology*, v. 141, p. 1–14.
- Morgan, D.J., Blake, S., Rogers, N.W., DeVivo, B., Rolandi, G., Macdonald, R., and Hawkesworth, C.J., 2004, Timescales of crystal residence and magma chamber volume from modeling of diffusion profiles in phenocrysts: Vesuvius 1944: *Earth and Planetary Science Letters*, v. 222, p. 933–946, doi: 10.1016/j.epsl.2004.03.030.
- Nakamura, M., 1995, Continuous mixing of crystal mush and replenished magma in the ongoing Unzen eruption: *Geology*, v. 23, p. 807–810, doi: 10.1130/0091-7613(1995)023<0807:CMOCMA>2.3.CO;2.
- Pan, Y., and Batiza, R., 2002, Mid-ocean ridge magma chamber processes: Constraints from olivine zonation in lavas from the East Pacific Rise at 9°30'N and 10°30'N: *Journal of Geophysical Research*, v. 107, p. 2022–2035, doi: 10.1029/2001JB000435.
- Petry, C., Chakraborty, S., and Palme, H., 2004, Experimental determination of Ni diffusion coefficients in olivine and their dependence on temperature, composition, oxygen fugacity, and crystallographic orientation: *Geochimica et Cosmochimica Acta*, v. 68, p. 4179–4188.
- Reid, M., 2003, Timescales of magma transfer and storage in the crust, in Holland, H.D., and Turkian, K.K., eds., *Treatise on geochemistry*, Volume 3: The crust: Oxford, Elsevier-Pergamon, p. 167–193.
- Shaw, C., 2004, The temporal evolution of three magmatic systems in the West Eifel volcanic field, Germany: *Journal of Volcanology and Geothermal Research*, v. 131, p. 213–240, doi: 10.1016/S0377-0273(03)00363-9.
- Spera, F.J., and Bohrsen, W.A., 2004, Open-system magma chamber evolution: An energy-constrained geochemical model incorporating the effects of concurrent eruption, recharge, variable assimilation and fractional crystallization (EC-E'RAXFC): *Journal of Petrology*, v. 45, p. 2459–2480, doi: 10.1093/petrology/egh072.
- Turner, S., Bourdon, B., and Gill, J., 2003, Insights into magma genesis at convergent margins from U-series isotopes, in Bourdon, B., et al., eds., *Uranium series geochemistry: Reviews in Mineralogy and Geochemistry*, v. 52, p. 255–315.
- White, R.A., 1996, Precursory deep long-period earthquakes at Mount Pinatubo: Pliotemporal link to a basalt trigger, in Newhall, C.G., and Punongbayan, R.S., eds., *Fire and mud: Eruptions and lahars of Mount Pinatubo*, Philippines: Seattle, University of Washington Press, p. 307–327.
- Zellmer, G.F., Blake, S., Vance, D., Hawkesworth, C., and Turner, S., 1999, Plagioclase residence times at two island arc volcanoes (Kameni Islands, Santorini, and Soufriere, St. Vincent) determined by Sr diffusion systematics: *Contributions to Mineralogy and Petrology*, v. 136, p. 345–357, doi: 10.1007/s004100050543.

Manuscript received 24 March 2005

Revised manuscript received 7 June 2005

Manuscript accepted 20 June 2005

Printed in USA